

RESEARCH

Open Access



# The degradation of poloxamer 188 in buffered formulation conditions

Wei Chen, Siegfried Stolz, Vincent Wegbecher, Dixy Parakkattel, Christina Haeuser, Nuria Sancho Oltra, Ravuri S. K. Kishore, Steven Bond, Christian Bell and Robert Kopf\*

## Abstract

Poloxamer 188 (P188) as a non-ionic surfactant is used in proteinaceous formulations to prevent protein adsorption to hydrophobic surfaces and unfolding at interfaces, preventing the formation of aggregates and particles. Its chemical intactness is crucial to the stability of drug products due to its protecting effects at interfaces. In order to identify and mitigate potential risks that might cause the degradation of P188 during the manufacturing process and storage, in the current work, the stability of P188 was investigated by forced degradation in buffered formulation conditions via oxidation and thermal stress conditions. The process of degradation was monitored through the dedicated liquid adsorption chromatography (LAC) with high sensitivity, and the degradants were characterized by high-resolution mass spectrometry. Results suggest that the vulnerability of P188 is largely related to the buffer conditions. Histidine promotes degradation in the presence of hydroxyl radicals but inhibits the degradation in the presence of H<sub>2</sub>O<sub>2</sub> and alkyl radicals. In thermal stress conditions, histidine protects P188 from degradation at 40 °C, and activates its decay only at higher temperature, like 60 °C.

**Keywords:** Poloxamer, Degradation, Chromatography, Pharmaceutically relevant conditions, Degradants characterization, LC-MS

## Introduction

Poloxamer as a polydisperse mixture of triblock copolymers was first developed by Lundsted and Ile (Lundsted and Ile 1954), and consists of one hydrophobic poly(propylene oxide) (PPO) block and two flanked hydrophilic poly(ethylene oxide) (PEO) chains with a molecular weight (Mw) ranging from a few thousand dalton (Da) up to 15 kDa. Because of its non-ionic structure and characteristic amphiphilicity, poloxamer was commercialized for emulsifying, thickening, coating, solubilizing, dispersing, and defoaming, with multiple grades varying in composition and molecular weight (Garcia Sagrado et al. 1994). Among a number of commercially available poloxamers, P188 was found suitable and was introduced into formulations to protect proteins from aggregating because of its decent biocompatibility, surfactant

property, and demonstrated chemical stability (Gu et al. 2013; Khan et al. 2015). These characteristics render P188 a promising alternative to polysorbates in overcoming the well-known hydrolysis issues of polysorbates (Kishore et al. 2011), and enable its application in commercial products, including Gazyva<sup>®</sup>, Orencia<sup>®</sup> (not all contain P188), Norditropin<sup>®</sup>, Enspryng<sup>®</sup>, and Hemlibra<sup>®</sup>.

Although independent thermal stress studies revealed the stability of P188 in solid state (Gallet et al. 2002; Erlandsson 2002), its susceptibility in a liquid formulation matrix comprising buffer components, salts, sugars, leachables, and extractables has been sparsely investigated. Only recently a report by Wang et al. unveiled the vulnerability of P188 in histidine buffer, in which the highly concentrated P188 solution ( $\geq 0.1\%$  (w/v)) underwent degradation after a 3-month incubation period at 40 °C, as evidenced by the change of pH, ultraviolet (UV) spectrum, chromatogram, and fluorescence (FL) spectrum (Wang et al. 2019). This

\*Correspondence: robert.kopf@roche.com  
F. Hoffmann-La Roche AG, Grenzacherstrasse 124, 4070 Basel, Switzerland

was explained by the assumption of the existence of histidine-derived radicals. Nevertheless, at low concentrations, P188 ( $\leq 0.04\%$  (w/v)) incubated under the same conditions remained stable, contradictory to the highly concentrated variant. We assume that the deviation in the results can stem from (i) the inadequate resolving power of the analytical methods to track the decay of the low concentration P188 or (ii) the accumulated impurities in the high concentration sample assisting the decomposition. To better understand the degradation process of P188 under pharmaceutical relevant conditions, this study investigated the impact of impurities on the P188 degradation in histidine buffer through a forced degradation study, including oxidation and thermal stress that may be encountered during the product life cycle. The decay was monitored through our recently developed liquid adsorption chromatography (Chen et al. 2021), with a shallow-gradient integrated for achieving high resolution, which allows close monitoring of the breakdown of P188 from each separated heterogeneous component. Besides that, the degradants were characterized through high-resolution mass spectrometry, and factors affecting the stability of P188 were proposed for future risk mitigation.

## Material and methods

### Reagents and materials

In all experiments, ultrapure water (specific resistance  $> 18.4 \text{ M}\Omega\text{-cm}$ ) was obtained from the Millipore Milli-Q purification system (Milli-Q Gradient A10, Kenilworth, NJ, USA). The chemicals and reagents were purchased from commercial suppliers and used directly without additional purification. Acetonitrile (ACN, Lichrosolv gradient grade for liquid chromatography), hydrochloric acid (25% for analysis), formic acid (98%), and sodium chloride were obtained from Merck KGaA (Darmstadt, Germany). L-histidine monochloride monohydrate (reagent grade 98%), ammonium acetate (reagent grade 98%), 2, 2'-Azobis (2-amidinopropane) dihydrochloride (AAPH, 97%), hydroperoxide (30%), polyethylene glycol (PEG) 1000, 2000, and 4000 (for synthesis) were purchased from Sigma-Aldrich (St. Louis, MO, USA). Ferric chloride hexahydrate (ACS grade) was obtained from MP Biomedicals (Solon, Switzerland). P188 (Kolliphor<sup>®</sup> P 188 Geismar, CoA is available in supplementary information) samples were acquired from BASF (Ludwigshafen, Germany) and dissolved in the corresponding solutions at 0.5 mg/mL before the stress study. A 10-mM PBS solution was prepared from the PBS tablets (Life Technologies Limited, Paisley, UK) by dissolving one tablet in 500 mL ultrapure water.

### Shallow-gradient chromatography for P188 analysis (LC-QDa)

A Waters ACQUITY UPLC I class System (Waters Corporation, Milford, MA, USA) equipped with a temperature controllable auto-sampler, a column compartment, and an isocratic solvent manager (ISM) was used to monitor P188 degradation. The temperature was set at 10 °C for the auto-sampler and at 65 °C for the column compartment. P188 components and its degradants were separated on the analytical column PLRP-S ( $50 \times 2.1 \text{ mm}$ , 5  $\mu\text{m}$ , 1000 Å) from Agilent Technologies (Santa Clara, USA) by the gradient shown in Table 1, with 0.05% formic acid aqueous solution as mobile phase A and 0.04% formic acid in ACN as mobile phase B; the flow rate was 0.2 mL/min. The entire elution was then neutralized by mixing with 5 mM ammonium acetate aqueous solution at 0.2 mL/min using the Waters Post Column Addition Kit, before entering the single quadrupole MS-detector (QDa Performance, Waters) in positive ion mode. The MS settings were as follows: cone voltage 80 V, source temperature 120 °C, positive capillary voltage 1.2 kV, negative capillary voltage 0.8 kV, probe temperature 600 °C, mass range 30–150 m/z, and sampling rate 5 points/s. For analysis, 1  $\mu\text{g}$  P188 samples were injected, and the data was processed by the selected ion mode with m/z 45 + 59 + 89 through the software Empower 3 (Waters, Milford, USA), in which substances eluting before 100.0 min were designated as degradants. The elution earlier than 110.0 min was termed as early eluters, and the later one from 110.0 till 135.0 min was termed as late eluters. The more late eluters, the more hydrophobic the P188 is. Although some degradants may co-elute with early/late eluters, their MS intensity is much lower than the P188, which was ignored in the calculation of degradation percentage by the relative peak area. The component

**Table 1** Gradient program of analytical chromatography

Time [min]	Eluent A [%]	Eluent B [%]
0.0	98	2
1.0	98	2
100.0	50	50
101.0	42	58
117.0	36	64
119.5	10	90
122.5	10	90
124.5	0	100
131.0	0	100
133.0	98	2
145.0	98	2

percentage was calculated from peak area of degradants, early eluters, and late eluters.

#### Sample preparation for forced degradation study

In the thermal stress study, 0.5 mg/mL P188 in PBS and histidine buffer at pH 6.0 was prepared, then divided into 0.5 mL aliquots placed into 1 mL screw neck HPLC vials to prevent potential contamination introduced by future sampling procedures. Vials were not filled with nitrogen. All vials were closed tightly with a polytetrafluoroethylene-coated cap (Waters Corporation, Milford, MA, US) and kept away from light. Initial (T0) samples were analyzed immediately after buffer preparation and the remaining vials were placed in the climate room at 40 °C/75% RH or incubated at 60 °C. The vials at 40 °C were analyzed at the timepoints 1, 3, and 6 months, and the vials at 60 °C were analyzed at the timepoints 2, 4, 6, and 8 weeks. Vials were retrieved accordingly and chilled rapidly in an ice bath before analysis.

In the oxidation stress study, the P188 buffer was prepared by mixing the corresponding amount of P188 into the stress buffers listed in Table 2 at a final concentration of 0.5 mg/mL and aliquoted into HPLC vials as previously described. Fenton was prepared by mixing the FeCl<sub>3</sub> with 0.1% H<sub>2</sub>O<sub>2</sub> in the corresponding buffers. Vials were not filled with nitrogen.

The freshly prepared samples were analyzed immediately, however, due to the fast degradation of P188, the results were not representative of the initial compositions. Therefore, the composition of thermal stress samples at the initial timepoint was considered to as the T0. The rest of the oxidation samples were stored in the climate room at 25 °C/60% RH and analyzed after 1, 2, 4, 6, and 8 weeks. In control reactions, P188 was incubated in buffers without oxidants/heating and processed in the same way as the stressed samples. No degradation was observed during the experiments. Data (Fig. S1) were shown in the supplementary information. In all cases, blank control solutions were incubated and analyzed under the same conditions in the event of interference with the analysis.

#### P188 fractionation via preparative HPLC

To characterize P188 degradants, one representative fraction of P188 was isolated from the entire polymer through the preparative HPLC (Waters e2695 HPLC)

equipped with the Waters Fraction Manager Analytical (WFMA). Separation was achieved on the Agilent Technologies PLRP-S column (250 × 4.6 mm, 8 μm, 1000 Å) at 65 °C according to the gradient shown in Table 3. Samples were collected at a flow speed of 1.5 mL/min, with water as mobile phase A and ACN as mobile phase B.

#### Lyophilization of P188 fractions

Fractions from preparative LC were freeze-dried with the SMH90 Lyophilizer (Usifroid, Maurepas, France). The solution was first transferred into sterilized standard 6 mL (ø 22-mm type I) clear glass vials (Schott forma vitrum AG, St. Gallen, Switzerland) and semi-stoppered with Teflon® coated stoppers (Daikyo Seiko, Tokyo, Japan). After 3 h frozen at −40 °C, primary drying occurred at −25 °C and 80 μbar for 26 h, followed by a secondary drying at 25 °C and 80 μbar for another 6 h. The condenser surface temperature was kept at −40 °C during the entire process. The resulting vials were stoppered and sealed with an aluminum crimp cap then stored at 2–8 °C for further studies.

#### Liquid chromatography-high-resolution mass spectrometry (LC-HRMS)

The analysis of P188 degradants was performed on a Agilent Technologies (Santa Clara, USA) PLRP 50 × 2.1 mm column, packed with 1000 Å pore size, 5 μm particles, connected to a Finnigan Orbitrap Fusion Lumos mass spectrometer (Thermo Scientific, USA). The column was operated at 65 °C and a flow rate of 0.2 mL/min on a Thermo Vanquish UPLC system (Waltham, USA).

**Table 3** Gradient program of P188 fractionation

Time [min]	Eluent A [%]	Eluent B [%]
0.0	50	50
10.0	50	50
235.0	36	64
245.0	0	100
255.0	0	100
265.0	50	50
280.0	50	50

**Table 2** The table of oxidants components and concentration

	Stress type	Compound	Concentration	Buffer system
Case I	Oxidation	Hydrogen peroxide	0.1% (w/v)	10 mM PBS or 10 mM histidine (pH 6.0)
Case II	Oxidation	FeCl <sub>3</sub>	20 ppm	
Case III	Oxidation	Fenton	0.1% (w/v)	
Case IV	Oxidation	AAPH	0.1% (w/v)	

The fractions of P188 and its degradants were eluted by the gradient shown in Table 1 using 20 mM ammonia in water as solvent A and 20 mM ammonia in ACN as solvent B. Typically, 1- $\mu$ g samples were loaded onto the column. Electrospray ionization was used as the ionization method and operated in positive mode. Samples were analyzed at full-scan mode from  $m/z$  250 to 2000. The other parameters used for the MS were the following: electrospray voltage 3500 V, ion transfer tube temperature 375 °C, vaporizer temperature 275 °C, orbitrap resolution 120,000. Xcalibur software was used for the qualitative and quantitative analysis.

## Results and discussion

P188 as a non-ionic surfactant composed of polyoxyalkane (PEO, PPO) chains plays a crucial role in protecting proteinaceous formulations at interfaces. However, PEO and PPO are susceptible to auto-oxidation owing to the presence of oxygen in the backbone, which activates the degradation process, and consequently affects its performance in formulations in terms of pH, surfactancy, and appearance (Donbrow 1987). Several publications implied the stability of P188 is dependent on its physical state and environment (Gallet et al. 2002; Erlandsson 2002; Wang et al. 2019). This raised our interests to study the likely factors influencing the stability of P188 in histidine buffer that is widely applied in proteinaceous formulations. These investigations were aided by liquid adsorption chromatography (LAC) with an unparalleled sensitivity.

### Liquid adsorption chromatography

Although several stability-indicating methods have been reported to monitor the degradation of P188 in terms of appearance, pH, aldehyde formation, and molar mass change, their application was limited to the apparent alterations of bulk materials in the storage (Erlandsson 2002). Approaches to understand the cleavage of P188 ( $\leq 0.05\%$  w/v) in the pharmaceutical practice from a

molecular perspective are still not fully explored. This arises from the limited separation power of conventional analytical methods to resolve the degradants from the complexity of superimposed heterogeneous constituents of P188. As P188 is composed of PEO and PPO, a chromatography capable of monitoring their cleavages unambiguously would be ideally suited for this purpose. In our previous P188 study (Chen et al. 2021), a LAC was developed to distinguish PPO block length in the single PO unit deviation. In this study, it was integrated with a shallow-gradient allowing differentiation of single EO unit variances, termed LC-QDa. By this means, the changes of both components of P188 could be chromatographed, as depicted in Fig. 1.

In this chromatogram, the gradient from 100 to 124.5 min is dedicated to resolve the PPO unit distribution. Each peak represents one type of P188 component containing a specific number of PO units. Cleavage on the PPO backbone will alter its affinity to the stationary phase, resulting in the shift of the chromatogram profile and change of the signal intensity. The degraded PEO and PPO-related substances can be resolved in the gradient from 1 to 100 min, which was indicated by the consecutive elution of PEO with  $M_w \sim 1000, 2000, \text{ and } 4000$ , appearing as multiple peaks. Each of them contains a concrete number of EO units. Therefore, this LC-QDa allows monitoring of the PEO-related species and the changes in the PPO block of P188 simultaneously, along with the semi-quantification of degradants using relative peak area.

### Forced degradation study of P188

Using the LC-QDa, the degradation of P188 in histidine solution was investigated under five stress conditions (Table 2), including the hydrogen peroxide, ferric ion, Fenton, AAPH, and thermal stress at 40 °C, all of which could occur in DP. The trace amount of hydrogen peroxide might be introduced from the residues in the aseptic filling process (Hubbard et al. 2018), or originating from

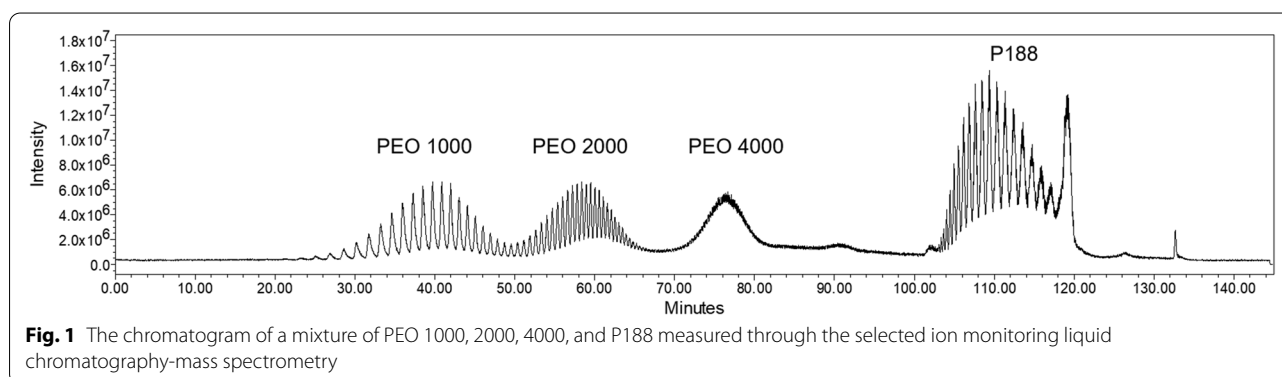
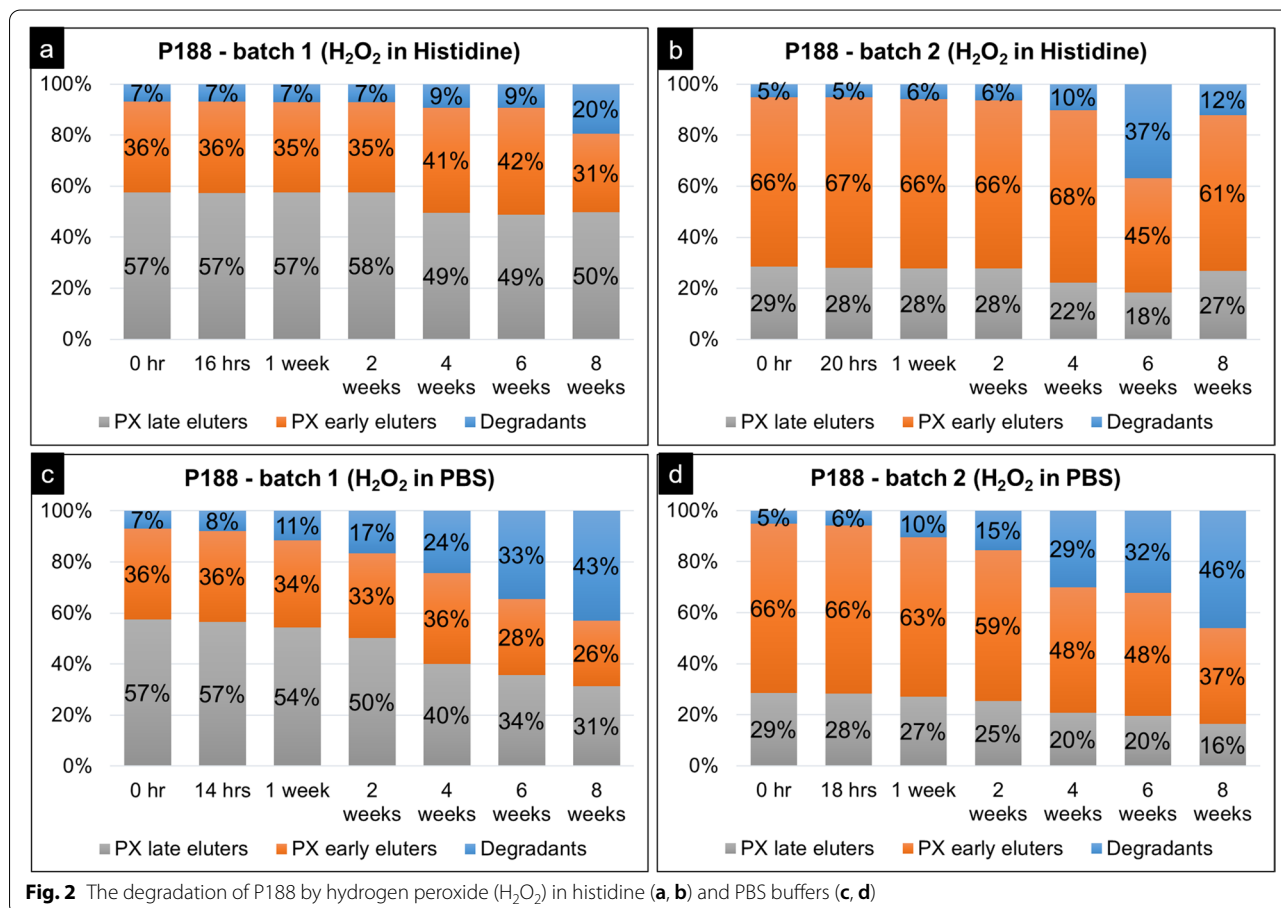


**Fig. 1** The chromatogram of a mixture of PEO 1000, 2000, 4000, and P188 measured through the selected ion monitoring liquid chromatography-mass spectrometry

the water vapor that condensed on the low-temperature surfaces in the freeze-thaw cycle or cold storage environment (Lee et al. 2020; Lee et al. 2019). The ferric ion, which can activate molecular oxygen to attack chemical compounds, can be incorporated as an impurity of the excipients, and as leachables/extractables from directly contacted surfaces (Taqi Khan and Martell 1967). Additionally, the combination of hydrogen peroxide and ferric/ferrous ion results in a Fenton condition that actively degrades the organic compounds via the hydroxyl radicals present (Zepp et al. 1992; Malik and Saha 2003). AAPH works as a radical initiator that stimulates the autoxidation of P188 known as a general degradation pathway of polyoxyalkylene (Yao et al. 2009). Finally, the thermal stress of P188 at 40 °C was examined to understand the impact of temperature deviation on P188 stability during shipment and storage as an extreme scenario. The degradation of P188 in PBS and histidine buffers at pH 6.0 was investigated under the same conditions. Two batches of P188 with varying amounts of hydrophobic subspecies (different late eluters percentage) were employed in the studies in case of variances in the results induced by the deviation of batch quality.

**Model stress case I: H<sub>2</sub>O<sub>2</sub>**

Under this condition, P188 was incubated with hydrogen peroxide in both histidine and PBS buffers. Batch 1 consisted of 7% degradants (blue bar), 36% early eluters (orange bar) and 57% late eluters (gray bar). Batch 2 was composed of 5% degradants, 66% early eluters, and 29% late eluters at the original state. As shown in Fig. 2, both P188 batches underwent degradation, although the degradation rate depended on the type of buffer. P188 was more stable in histidine (Fig. 2a, b) compared to PBS (Fig. 2c, d), in which the polymer remained intact up to 2 weeks, and only experienced 9% percent degradation in the first 4 weeks, while the degradation of the counterpart in PBS commenced during the first 14–18 h, and increased to more than 40% within 8 weeks. Although the maximum degradation in histidine was observed to be 20% in batch 1 (at 8 weeks in Fig. 2a), batch 2 showed an unexpected fluctuation from 10 to 37% (at 6 weeks in Fig. 2b), followed by a decrease to 12% in the following weeks. After careful examination, we confirmed that the deviation was not caused by the artifacts of analysis, but more likely due to rapid oxidative degradation of the specific sample itself likely due to contamination in the



sample. The 8w sample is however in line with the trend seen.

**Model stress case II: Fe<sup>3+</sup>**

As the product can be contaminated by metal ions from multiple sources, such as the leachable from containers and impurities of excipients, the effect of Fe<sup>3+</sup> on P188 degradation was investigated. The results demonstrated that neither in histidine buffer nor in the PBS matrix was Fe<sup>3+</sup> detrimental to P188, as the polymer remained intact after eight weeks of incubation (data not shown). This can be attributed to the unsuccessful formation of oxygen-derived species from the endogenous hydroperoxide or dissolved molecular oxygen as reported before (Kerwin 2008).

**Model stress case III: H<sub>2</sub>O<sub>2</sub> + Fe<sup>3+</sup>**

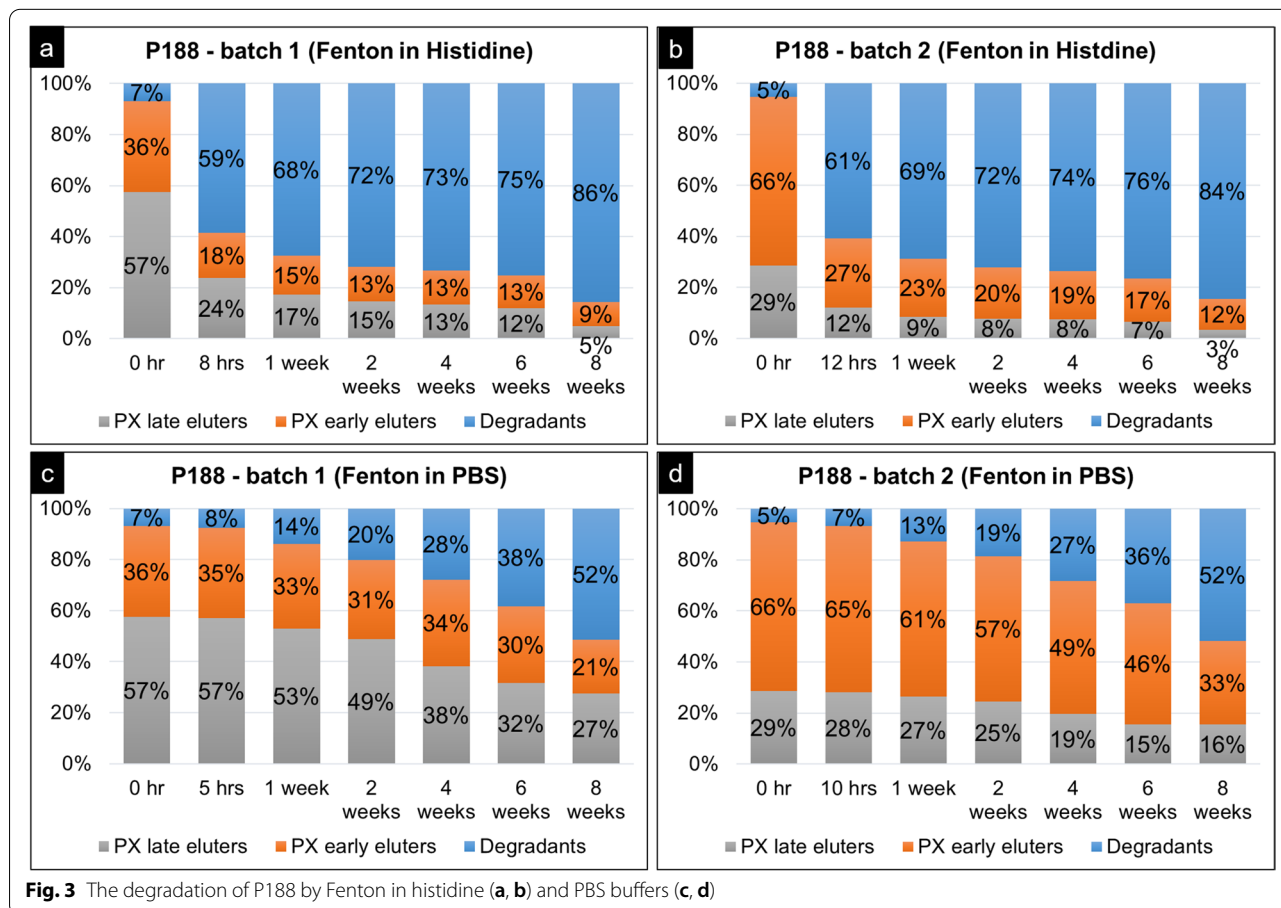
It is known that the combination of ferric iron with hydrogen peroxide will trigger the Fenton reaction/Haber-Weiss cycle (Haber and Weiss 1932), and the resulting hydroxyl radicals are highly reactive to organic compounds. In order to study its effect on P188, Fe<sup>3+</sup> instead of Fe<sup>2+</sup> was mixed with H<sub>2</sub>O<sub>2</sub>, because it is more

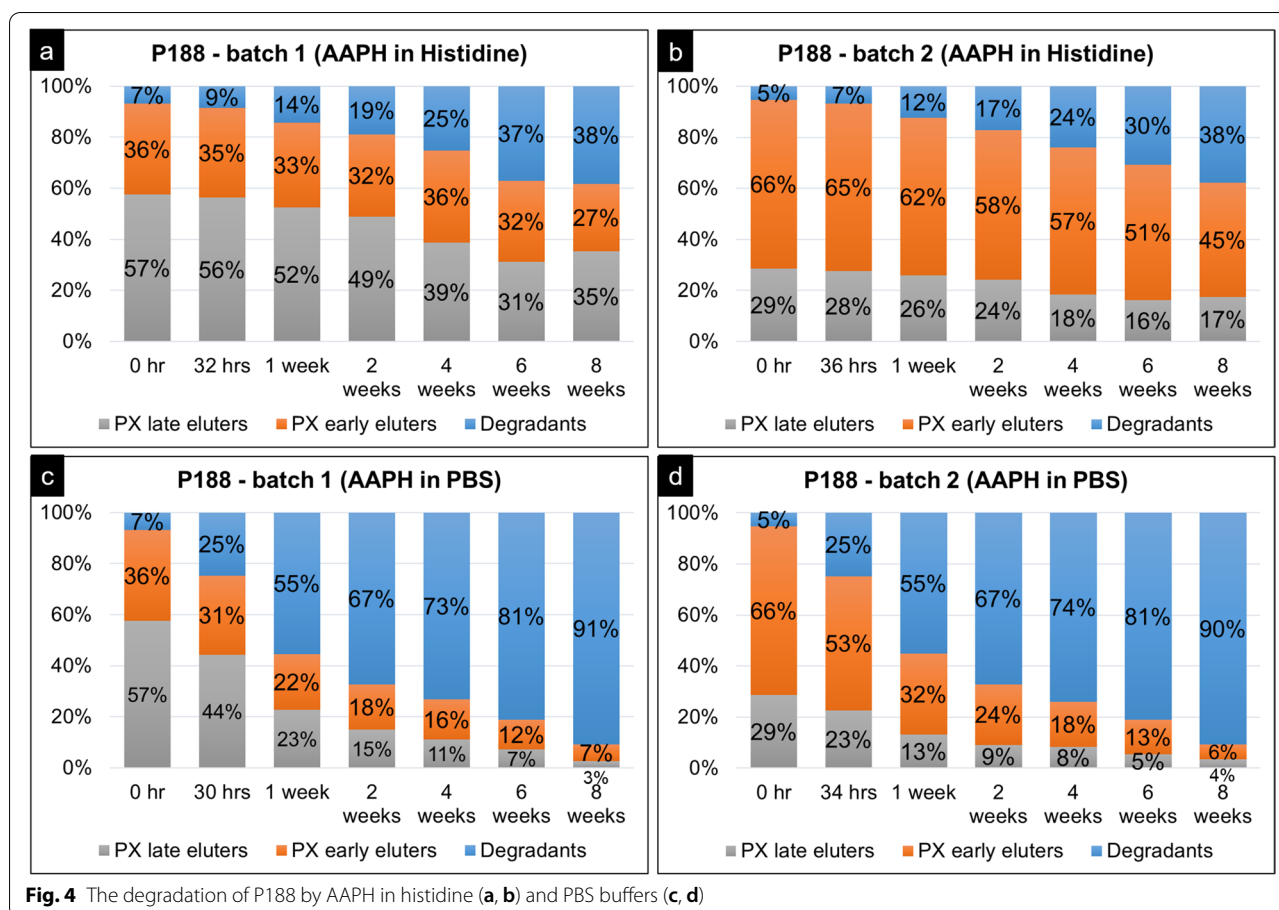
likely to appear during the manufacturing process. As a result, a substantial cleavage of P188 was observed in both buffers, where histidine accelerated the degradation more severely than PBS, as shown in Fig. 3. The degradants of both batches in histidine buffer (Fig. 3a, b) surged to ~60% within 8–12 h, then increased to ~85% within 8 weeks in histidine containing formulation, while the degradants in PBS buffer (Fig. 3c, d) reached only ~10% and 52%, respectively, over the same time period.

**Model stress case IV: AAPH**

The dependence of P188 degradation on buffer types was also observed in the AAPH condition. Histidine appeared to attenuate the decomposition of P188 as shown in Fig. 4, where only an additional 7% degradants were generated in the first week, while an additional ~50% degradants were produced in PBS. Further incubation led to one-third degradation of P188 in histidine buffer and 90% decay in PBS solution within 8 weeks, demonstrating the buffer media influencing the degradation process.

As displayed by the above data, the degradation of P188 induced by different oxidation agents varied dramatically according to media, in which histidine played the role

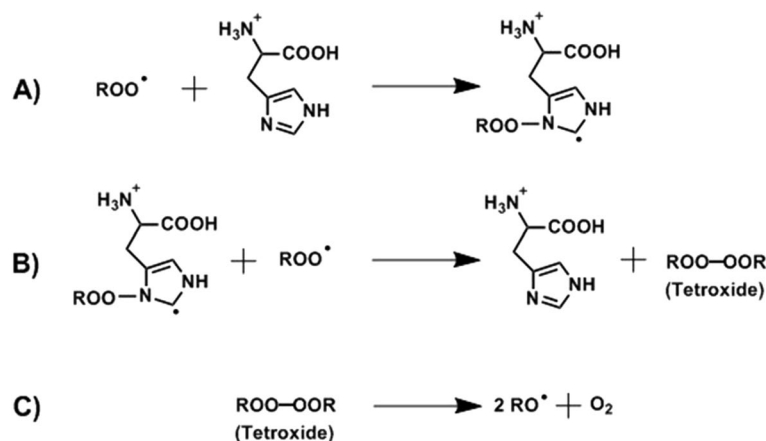




of either catalyzing or inhibiting the degradation. This might arise from the known property of histidine functioning either as a scavenger of reactive oxygen/nitrogen species (Mori et al. 2020; Holeček 2020), or a radical reaction center, like non-heme iron-containing enzymes, to catalyze oxidation (Karlin 1993). In our study, histidine behaved as a scavenger under  $H_2O_2$  and AAPH conditions, and as a catalyst in Fenton condition. With respect to the hydrogen peroxide (Case I), the oxidation is believed to take place primarily through the nucleophilic reaction in a manner of peroxide-protic solvent complex (Li et al. 1995). Excessive histidine competitively reacted with  $H_2O_2$ , resulting in the protection of P188 by forming related oxidation products (Uchida 2003). However, the incorporation of metal ions sufficiently alter the reaction pathway (Case III), in which the ferric ion are first converted to  $Fe^{2+}$  with the aid of the superoxide anion ( $\cdot O_2^-$ ), then split one  $H_2O_2$  into two hydroxyl radicals ( $\cdot OH$ ). These freshly generated radicals form an adduct with the imidazole moiety of histidine forming the transient neutral histidine-radicals to facilitate the electron-transfer and oxidation of P188 such as the metalloenzymes and radical-enzymes (Lassmann et al. 2000).

With respect to the AAPH (Case IV), histidine plays the role of a trap that converts the reactive radicals to the mild ones (Nauser and Carreras 2014). In this condition, alkylperoxides ( $ROO\cdot$ ) are first generated via the decomposition of AAPH. Then the presence of histidine consume alkylperoxides ( $ROO\cdot$ ) through a process as shown in Scheme 1, in which the alkylperoxide radical ( $ROO\cdot$ ) are added to histidine, followed by a reaction with additional alkylperoxide ( $ROO\cdot$ ) to reconstitute histidine and the intermediary tetroxide. The unstable tetroxide consequently decomposed into oxygen and low reactive alkoxyl radicals ( $RO\cdot$ ) that is shown to react more preferably with histidine than polyoxyalkylene (Zhang et al. 2018).

Generally speaking, the reactivity of oxidants (without the influence of histidine) follows this order: AAPH >  $\cdot OH$  (Fenton) >  $H_2O_2$  in line with the physiological study (Winterbourn 1995). However, in the presence of histidine, the oxidative power of such species is altered as follows:  $\cdot OH$  (Fenton) > AAPH >  $H_2O_2$ . This might explain the fluctuation shown in Fig. 2b that the degradants of P188 increased to 37% in week 6 sample likely due to an induced Fenton reaction in the particular sample by the introduction of metal impurities. Additionally, under all



**Scheme 1** The illustration of the chemical reactions that alkylperoxides ( $\text{ROO}^\bullet$ ) originating from AAPH react with histidine (A), followed by the addition of second alkylperoxide ( $\text{ROO}^\bullet$ ) to reconstitute histidine and tetroxide (B), then the tetroxide decomposes to alkoxy radicals ( $\text{RO}^\bullet$ ) (C)

the stress conditions, the degradation took place equally on early eluters and late eluters as both batch 1 and 2 varied in the amount of early/late eluters, but resulted in almost equivalent amounts of degradants under the same stress condition. This observation indicated that the degradation of the polymeric chains was governed by statistical rupture at various sites regardless of hydrophobicity of the poloxamer components.

#### Thermal stress

A thermal stress study of P188 at 40 °C was additionally carried out to test the impact of temperature deviation on the formulation as an accelerating approach. Its impact on P188 was recorded as a function of time as shown in Fig. 5. P188 in PBS was more degraded than in histidine solution and exhibited an inconsistent degradation rate among samples. In Fig. 5c (batch 1), the degradants reached 26% after the first 3 months, and decreased slightly to 22% in the sixth month, whereas batch 2 (Fig. 5d) held 10% degradants for the first three months, then increased to 38% after a 6-month storage period. We propose such a discrepancy might be induced by the ppb level of iron ions (<100 ppb) in PBS that facilitate the autoxidation reactions by easing the formation of initial radicals through redox reactions with organic substrates (Heiba et al. 1969), molecular oxygen (Feig and Lippard 1994) or hydroperoxides (Goldstein et al. 1993). The level of iron ions was determined via inductively coupled plasma mass spectrometry (ICP-MS) with the quantification limit of 100 ppb as reported before (Ditter et al. 2018). Due to the low concentration of iron ion, the degradation is governed by the chance of its encounter with P188 and oxygen. As a result, the ignition of P188 autoxidation is, statistically speaking, exhibiting the variance of degradation among individual vials.

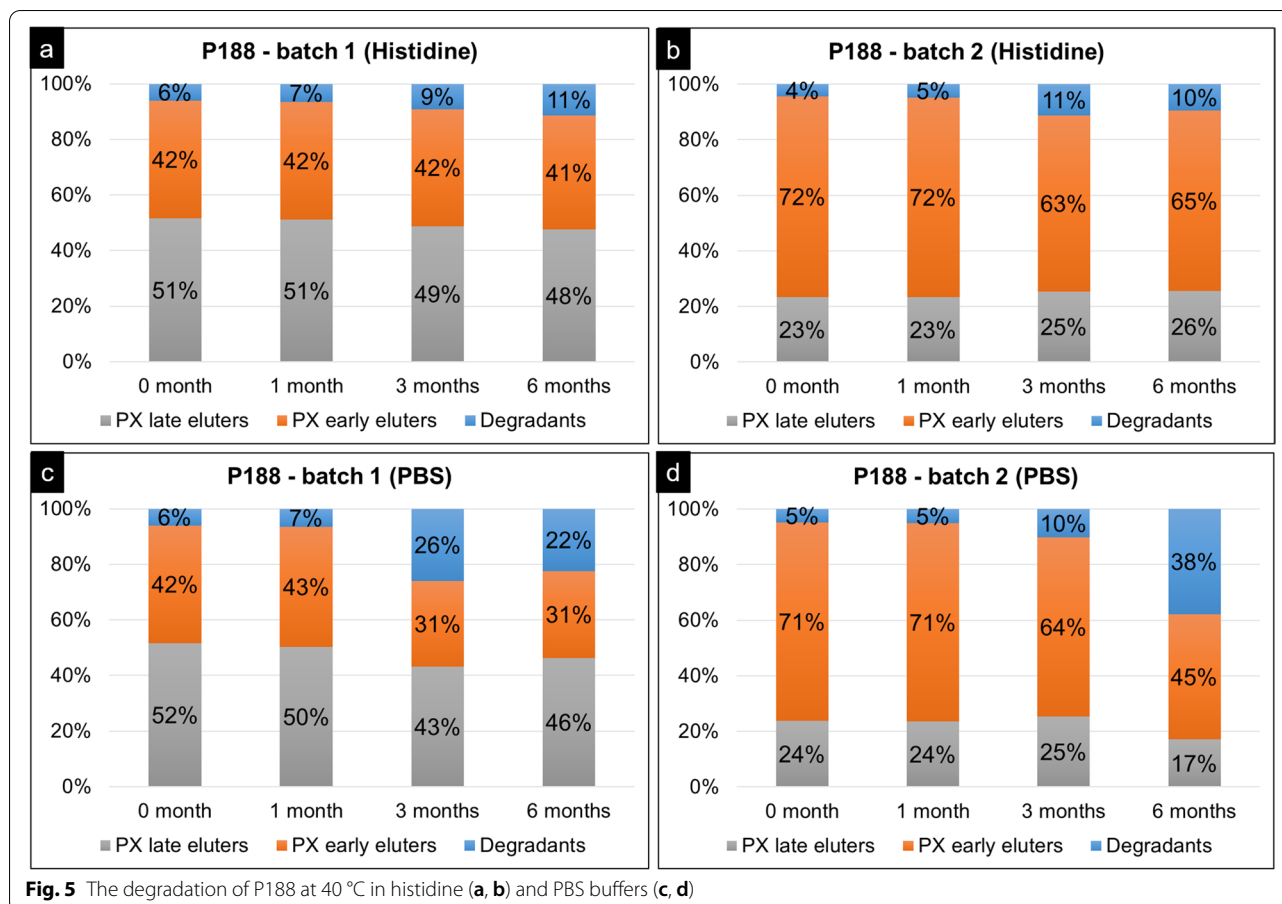
To further prove the scavenging capacity of histidine to autoxidation, we elevated the incubation temperature to 60 °C to generate peroxy radicals by facilitating the reaction of oxygen with P188.

In this experiment, P188 from batch 3 with similar early and late eluters percentage to batch 1 was employed as an alternative due to the shortage of batch 1. Contrary to our expectation, histidine accelerated the degradation of P188 instead of inhibiting it. As shown in Fig. 6a, degradants reached 41%, whereas the counterparts in PBS achieved only 32% (Fig. 6c) after 8 weeks of incubation. Remarkably, the degradants in histidine buffer originated primarily from late eluters rather than early eluters. As depicted in Fig. 6a, late eluters contributed 32% of total degradants, while early eluters accounted for only 3%. However, this cleaving propensity did not appear in the PBS buffer, in which degradants increased approximately evenly from early/late eluters (Fig. 6c, d). Considering the thermal oxidation and cleavage of polyoxyalkane (PEO, PPO) should be a random process (Griffiths et al. 1993), the affinity to late eluters might be attributed to the histidine-derived radicals generated at 60 °C (Jeffrey et al. 2008). This also explained the fewer degradants appearing in batch 2 (Fig. 6b) than in batch 3 (Fig. 6a). As batch 2 comprised nearly two times fewer late eluters than those of batch 3, the attack of histidine-derived radicals was kinetically unfavorable. It is noteworthy that this degradation propensity was only observed in histidine buffer at 60 °C, which points to thermally derived radicals process.

#### P188 degradation characterization

Taking into account of the inevitable ferric ion and oxygen in the manufacturing process, as well as the histidine buffer used in the formulation, the decomposition



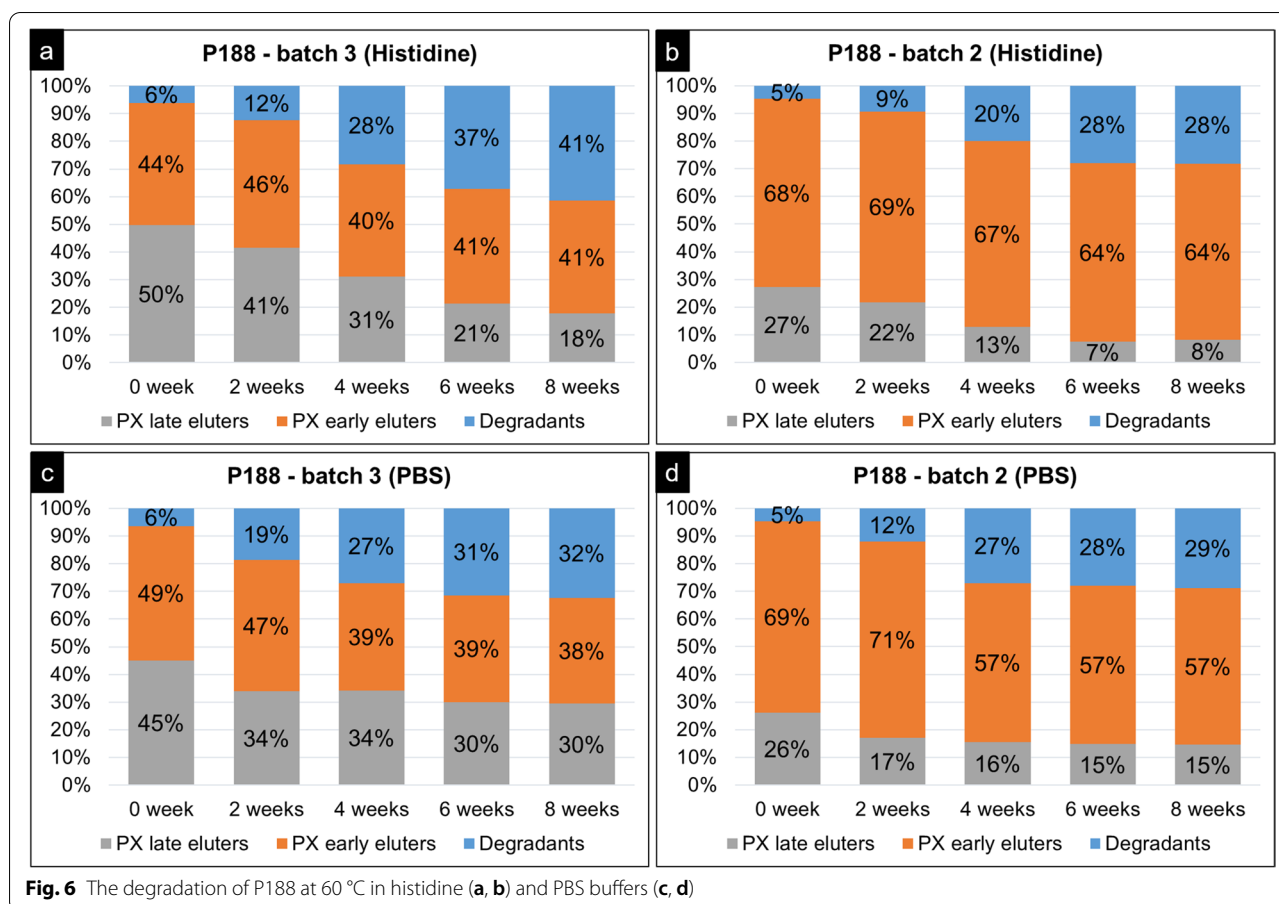


of P188 was investigated by incubating one fraction of P188 in the histidine–Fenton condition for 24 h and subsequent analysis of the degraded residue by means of LC-HRMS. The advantage of analyzing one fraction instead of the intact P188 is that it contains all building blocks, but with narrowly distributed PPO/PEO chains, therefore minimizing the complexity of MS spectra without compromising the representativeness of the sample.

As shown in Fig. 7, the chromatogram before degradation consists primarily of two elution peaks at 113.9 min and 112.8 min, whereas three groups of additional peaks emerged in the retention times (RT) ranging from 0 to 80 min (Group 1), from 102 to 112 min (Group 2), and from 120 to 125 min (Group 3) after 24 h of degradation. Based on the separation mechanism, Group 1 is attributed to the PEO-related substances, Group 2 belongs to substances resulting from PPO cleavage, and Group 3 is composed of more hydrophobic components from the P188 fractions. More chemical information can be obtained from their mass spectrum.

As shown in Fig. 8, Group 1 exhibited six well-resolved mass series corresponding to the PEO species containing different EO units and charges that

were adducts with either ammonium or trace residual amylamine ( $C_5H_{13}N$ ) and hexylamine ( $C_6H_{15}N$ ) from other experiments. The first mass series from RT of 10 min represented single-charged EO oligomers and the number of charges increased by one along the adjacent series. The inspection of the inset expansion indicated that two species are present in the samples marked as A and B. The series A at  $m/z$  414.3 can be assigned to the  $(EO)_7$  with an amylammonium adducted. The series B located at  $m/z$  416.3 is an analog to series A, but shorter by one  $CH_2$  and larger by one O. Their presence can be accounted for by the degradation of the PEO chain via the alkoxy radical that underwent  $\beta$ -scission to cleave C–O or C–C (Santacesaria et al. 1991). The additional O atom in series B might be caused by the quenching of alkoxy radical via inter- or intramolecular hydrogen abstraction, leaving one more OH group on the polymer chain. The other ions in the spectrum are derived from different ion adducts on the same EO series. The deconvoluted mass of the multi-charged PEO fragments was found between approximately 300 Da and 4500 Da, which agrees with the theoretical PEO distribution of P188.



Although LC-HRMS is able to provide insights into the possible degradants, the analysis of Group 2 (RT 102–112 min) was not feasible. Because of the low ion abundance of these species, the lack of the obvious ion pattern for analysis, and the convoluted multi-charged ions, the challenge to deduce their chemical structures increased. However, based on the fragmentation data from LC-QDa, the PPO fragment with specific  $m/z$  59 was observed, which supported the assignment of Group 2 to PPO-related degradants. The sharp peak observed at 102.72 min was caused by gradient change. To further characterize these degradants, matrix-assisted laser desorption ionization-time of flight mass spectrometry (MALDI-TOF MS) will be carried out in a future effort.

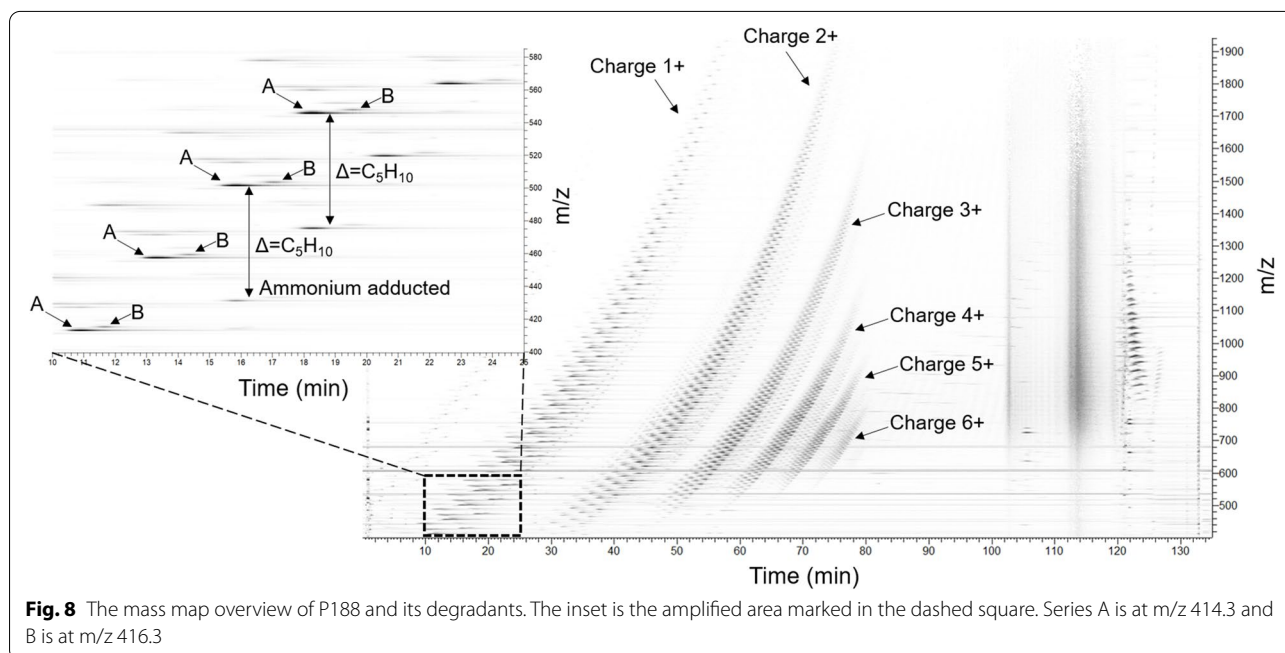
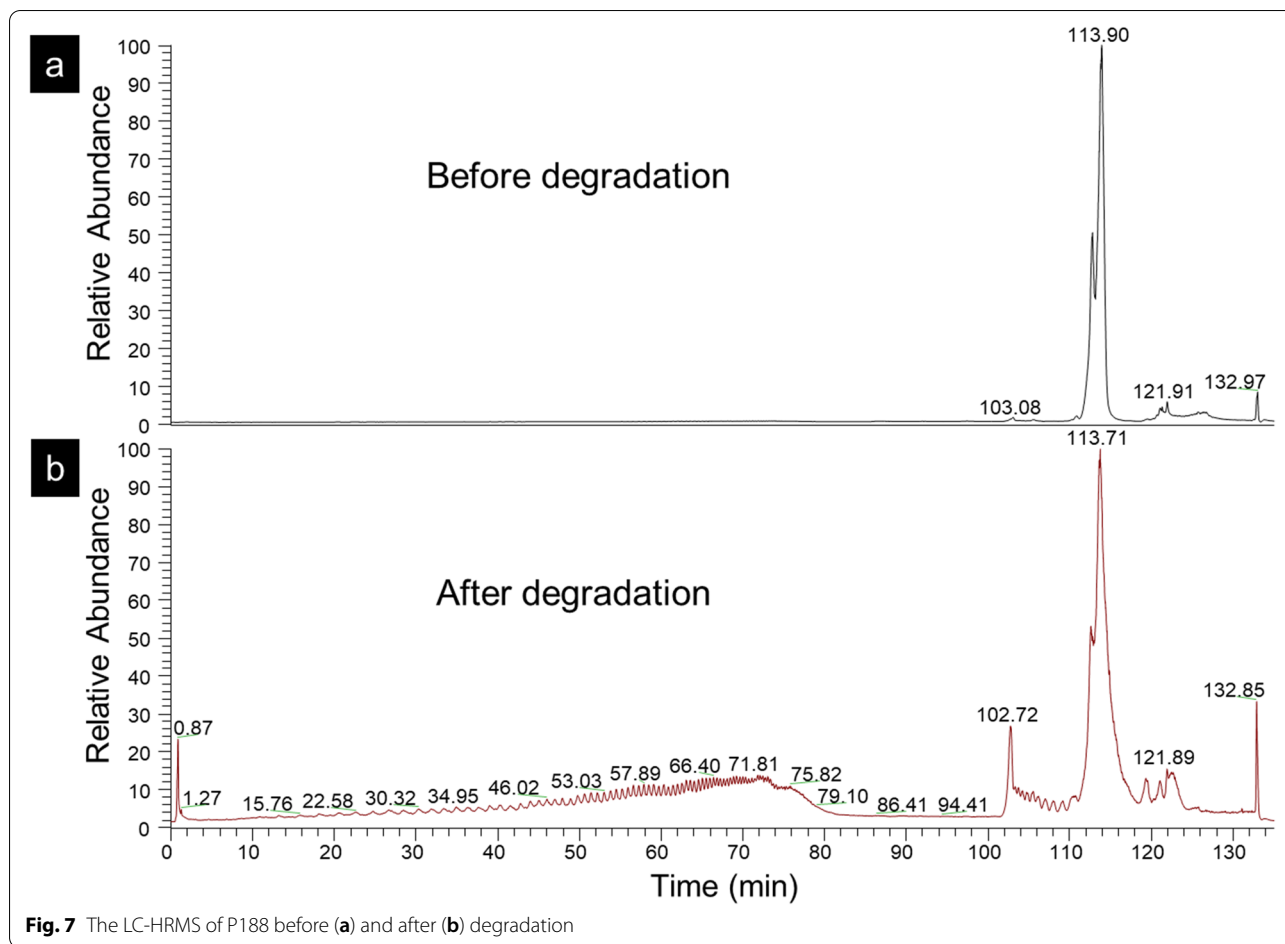
The MS results of Group 3 (RT 120–125 min) further demonstrated the existence of PPO residue. The peaks from RT 120.5–121.2 min displayed a 3+ charged homologous series of PPO on the mass spectrum (Fig. 9). The peak at RT 120.8 min exhibited  $m/z$  797.92914 and was identified as  $(\text{PO})_{40}$  with three  $\text{NH}_4^+$  adducted. Considering the fraction of P188 used in the forced degradation only contained 29 units of PO, the compound with the higher molecular weight might be presumably caused by

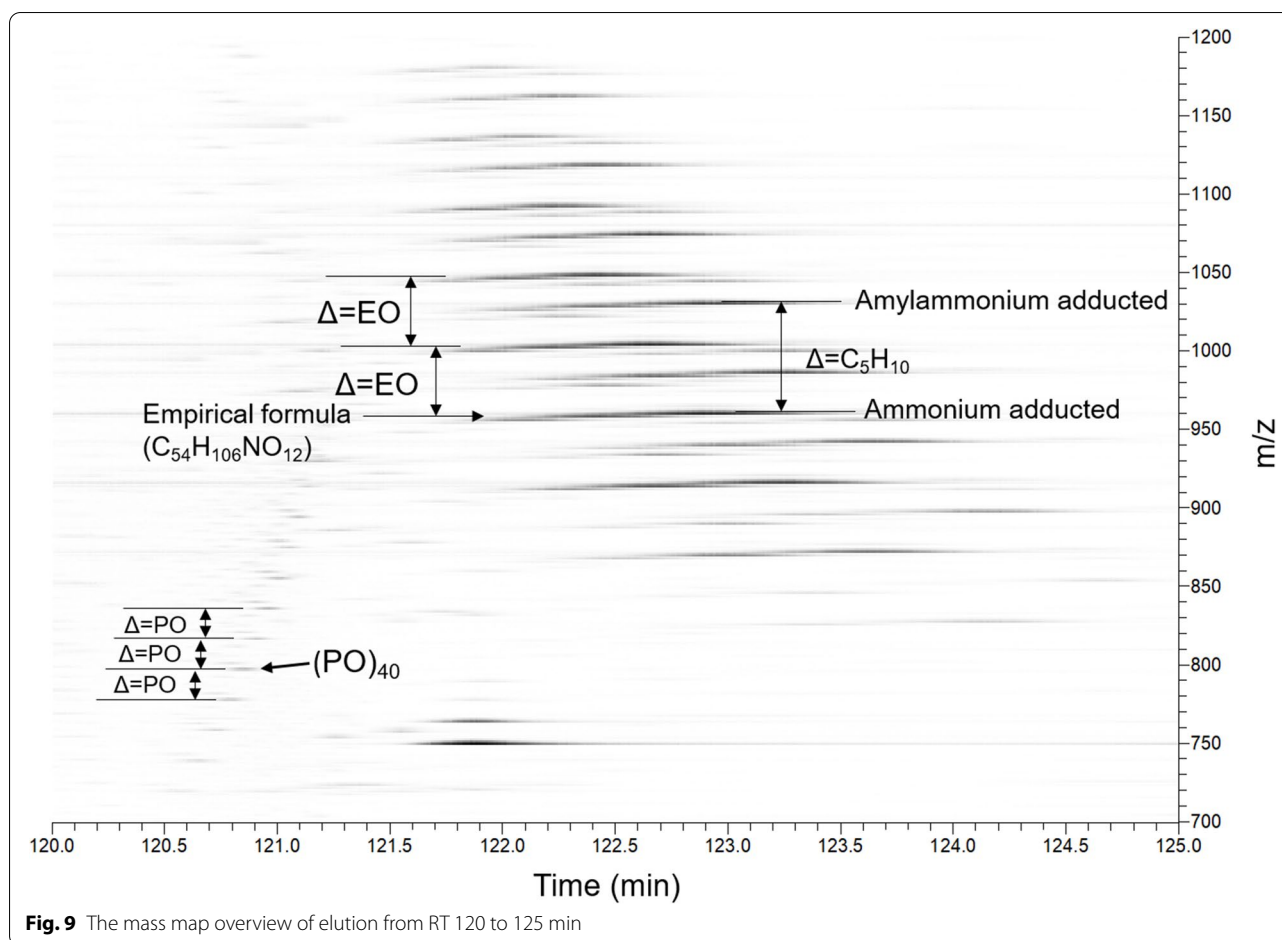
the radical coupling of two PPO fragments. The driving force facilitating the occurrence can be explained by the hydrophobic interaction of PPO fragments. This interaction would bring fragments in the vicinity resulting in an efficient coupling. Other homologs were also observed at RT 122–124 min. Although the mass difference between the individual homologs is 44 Da (one EO unit), the proposed empirical formula ( $\text{C}_{54}\text{H}_{106}\text{NO}_{12}$ ) can not match the derivatives from PEO or PPO due to the deficiency of oxygen in the formula.

Although the LC-HRMS measurements were unable to detect the volatile compounds like organic acids, aldehydes and acetone, these compounds should also be part of the degradants that were generated from the  $\beta$ -scission and six-ring intramolecular decomposition reaction (Kishore et al. 2011). Detailed evaluation of these species was beyond the context of this study that focused on the degraded oligomers from P188.

## Conclusion

The degradation of P188 was investigated through five stress conditions, including  $\text{H}_2\text{O}_2$ ,  $\text{Fe}^{3+}$ , Fenton, AAPH at 25 °C, and a temperature of 40 °C, to simulate the





potential residual impurities, contaminations, and the worst-case temperature deviations experienced by DP. The degradation results suggested that P188 reacts differently according to its buffer environment. Histidine as a common buffer agent used in protein formulation was found to be actively detrimental to P188 in the Fenton condition, but protective in  $\text{H}_2\text{O}_2$ , AAPH, and at 40 °C. The results point to the benefit of using histidine buffers in combination with P188 as a surfactant in controlling the risk of radical derived degradation of P188.

#### Abbreviations

AAPH: 2, 2'-Azobis (2-amidinopropane) dihydrochloride; ACN: Acetonitrile; Da: Dalton;  $\text{FeCl}_3$ : Ferric chloride; FL: Fluorescence; HMW: High-molecular-weight; LC: Liquid chromatograph; HRMS: High-resolution mass spectrometry; HPLC: High-performance liquid chromatography;  $\text{H}_2\text{O}_2$ : Hydrogen peroxide; ISM: Isocratic solvent manager; LAC: Liquid adsorption chromatograph; Mw: Molecular weight; MALDI-TOF MS: Matrix-assisted laser desorption ionization-time of flight mass spectrometry; P188: Poloxamer 188; PPO: Poly(propylene oxide); PEO: Poly(ethylene oxide); PBS: Phosphate-buffered saline; RT: Retention time; RH: Relative humidity; UV: Ultraviolet; WFMA: Waters fraction manager analytical.

#### Supplementary Information

The online version contains supplementary material available at <https://doi.org/10.1186/s41120-022-00055-4>.

**Additional file 1:** The online version contains supplementary material. **Table S1.** The P188 certificate of analysis (CoA). **Figure S1.** The degradation profile of P188 in histidine (a, b) and PBS buffers (c, d).

#### Acknowledgements

We would like to thank Margot Reth, Valerie Wuertz, and Covadonga Palacio for the ICP-MS measurements.

#### Authors' contributions

WC and RK conceptualized the research work, investigated, curated the data, drafted and edited the original draft. SS conducted the MS analysis, interpreted data, and drafted the manuscript. VW conducted the lyophilization. DP provided the buffers and prepared samples. CH, NO, SR, and SB reviewed and edited the draft. CB administrated the project and reviewed and edited the draft. The authors read and approved the final manuscript.

#### Funding

Not applicable

#### Availability of data and materials

All data generated or analyzed during this study are included in this published article.

## Declarations

### Competing interests

The authors declare that they have no competing interests. The contents of this manuscript have not been presented previously at any scientific conference or published in any conference proceeding.

Received: 10 September 2021 Accepted: 3 March 2022

Published online: 21 March 2022

## References

- Chen W, Ross A, Steinhuber B, Hoffmann G, Oltra NS, Kishore RS, Bond S, Bell C, Kopf R (2021) The development and qualification of liquid adsorption chromatography for poloxamer 188 characterization. *J Chromatogr A* 1652:462353. <https://doi.org/10.1016/j.chroma.2021.462353>
- Ditter D, Nieto A, Mahler HC, Roehl H, Wahl M, Huwyler J, Allmendinger A (2018) Evaluation of delamination risk in pharmaceutical 10 mL/10R vials. *J Pharm Sci* 107:624–637. <https://doi.org/10.1016/j.xphs.2017.09.016>
- Donbrow M (1987) Stability of polyoxyethylene chain in nonionic surfactants. *Nonionic surfactants: Physical chemistry*, vol 23. CRC Press, New York
- Erlandsson B (2002) Stability-indicating changes in poloxamers: the degradation of ethylene oxide-propylene oxide block copolymers at 25 and 40 °C. *Polym Degrad Stab* 78:571–575. [https://doi.org/10.1016/S0141-3910\(02\)00233-1](https://doi.org/10.1016/S0141-3910(02)00233-1)
- Feig AL, Lippard SJ (1994) Reactions of non-heme iron (II) centers with dioxygen in biology and chemistry. *Chem Rev* 94:759–805. <https://doi.org/10.1021/cr00027a011>
- Gallet G, Carroccio S, Rizzarelli P, Karlsson S (2002) Thermal degradation of poly(ethylene oxide-propylene oxide-ethylene oxide) triblock copolymer: comparative study by SEC/NMR, SEC/MALDI-TOF-MS and SPME/GC-MS. *Polymer* 43:1081–1094. [https://doi.org/10.1016/S0032-3861\(01\)00677-2](https://doi.org/10.1016/S0032-3861(01)00677-2)
- Garcia Sagrado F, Guzman M, Molpeceres J, Aberturas MR (1994) Pluronic copolymers - characteristics, properties and pharmaceutical application: part II. *Pharmaceutical Technology Europe*:38–44
- Goldstein S, Meyerstein D, Czapski G (1993) The Fenton reagents. *Free Rad Biol Med* 15:435–445. [https://doi.org/10.1016/0891-5849\(93\)90043-t](https://doi.org/10.1016/0891-5849(93)90043-t)
- Griffiths PJF, Hughes JG, Park GS (1993) The autoxidation of poly(propylene oxide)s. *Eur Polym J* 29:437–442. [https://doi.org/10.1016/0014-3057\(93\)90116-W](https://doi.org/10.1016/0014-3057(93)90116-W)
- Gu JH, Ge JB, Li M, Xu HD, Wu F, Qin ZH (2013) Poloxamer 188 protects neurons against ischemia/reperfusion injury through preserving integrity of cell membranes and blood brain barrier. *PLoS One* 8:e61641. <https://doi.org/10.1371/journal.pone.0061641>
- Haber F, Weiss J (1932) Über die Katalyse des Hydroperoxydes. *Naturwissenschaften* 20:948–950. <https://doi.org/10.1007/BF01504715>
- Heiba EI, Dessau RM, Koehl JW (1969) Oxidation of metal salts. V. Cobaltic acetate oxidation of alkylbenzenes. *J Am Chem Soc* 91:6830–6837. <https://doi.org/10.1021/ja01052a049>
- Holeček M (2020) Histidine in health and disease: metabolism, physiological importance, and use as a supplement. *Nutrients* 12:848–867. <https://doi.org/10.3390/nu12030848>
- Hubbard A, Roedel T, Hui A, Knueppel S, Eppler K, Lehnert S, Maa YF (2018) Vapor phase hydrogen peroxide decontamination or sanitization of an isolator for aseptic filling of monoclonal antibody drug product-hydrogen peroxide uptake and impact on protein quality. *PDA J Pharm Sci Technol* 72:348–366. <https://doi.org/10.5731/pdajpst.2017.008326>
- Jeffrey S, Zhao J, Siu C, Ke Y, Verkerk UH, Oomens J, Dunbar RC, Hopkinson AC, Siu KWM (2008) Structure of the observable histidine radical cation in the gas phase: a captodative  $\alpha$  - radical ion. *Angew Chem Int Ed* 47:9666–9668. <https://doi.org/10.1002/ange.200804101>
- Karlin KD (1993) Metalloenzymes, structural motifs, and inorganic models. *Science* 261:701–708. <https://doi.org/10.1126/science.7688141>
- Kerwin BA (2008) Polysorbates 20 and 80 used in the formulation of protein biotherapeutics: structure and degradation pathways. *J Pharm Sci* 97:2924–2935. <https://doi.org/10.1002/jps.21190>
- Khan TA, Mahler HC, Kishore RSK (2015) Key interactions of surfactants in therapeutic protein formulations: a review. *Eur J Pharm Biopharm* 97:60–67. <https://doi.org/10.1016/j.ejpb.2015.09.016>
- Kishore RS, Kiese S, Fischer S, Pappenberger A, Grauschopf U, Mahler HC (2011) The degradation of polysorbate 20 and 80 and its potential impact on the stability of biotherapeutics. *Pharm Res* 28:1194–1210. <https://doi.org/10.1007/s11095-011-0385-x>
- Lassmann G, Eriksson LA, Lenzian F, Lubitz W (2000) Structure of a transient neutral histidine radical in solution: EPR continuous – flow studies in a Ti3+/EDTA – Fenton system and density functional calculations. *J Phys Chem A* 104:9144–9152. <https://doi.org/10.1021/jp001437w>
- Lee JK, Han HS, Chaikasetin S, Marron DP, Waymouth RM, Prinz FB, Zare RN (2020) Condensing water vapor to droplets generates hydrogen peroxide. *Proc Natl Acad Sci* 117:30934–30941. <https://doi.org/10.1073/pnas.2020158117>
- Lee JK, Walker KL, Han HS, Kang J, Prinz FB, Waymouth RM, Nam HG, Zare RN (2019) Spontaneous generation of hydrogen peroxide from aqueous microdroplets. *Proc Natl Acad Sci* 116:19294–19298. <https://doi.org/10.1073/pnas.1911883116>
- Li S, Schoneich C, Borchardt RT (1995) Chemical instability of protein pharmaceuticals: mechanism of oxidation and strategies for stabilization. *Biotechnol Bioeng* 48:490–500. <https://doi.org/10.1002/bit.260480511>
- Lundsted LG, Ile, G. (1954) Polyoxylakylene compounds. United States Patent, 2674619.
- Malik PK, Saha SK (2003) Oxidation of direct dyes with hydrogen peroxide using ferrous ion as catalyst. *Sep Purif Technol* 31:241–250. [https://doi.org/10.1016/S1383-5866\(02\)00200-9](https://doi.org/10.1016/S1383-5866(02)00200-9)
- Mori A, Hatate H, Tanaka R (2020) Ability of three kind of imidazole dipeptides, carnosine, anserine, and balenine, to interact with unsaturated fatty acid-derived aldehydes and carbohydrate-derived aldehydes. *Int J Pept Res Ther* 26:1651–1660. <https://doi.org/10.1007/s10989-019-09975-4>
- Nausier T, Carreras A (2014) Carbon-centered radicals add reversibly to histidine – implications. *Chem Commun* 50:14349–14351. <https://doi.org/10.1039/c4cc05316h>
- Santacesaria E, Gelosa D, Serio MD, Tesser R (1991) Thermal stability of non-ionic polyoxyalkylene surfactants. *J Appl Polym Sci* 42:2053–2061. <https://doi.org/10.1002/app.1991.070420733>
- Taqi Khan MM, Martell AE (1967) Metal ion and metal chelate catalyzed oxidation of ascorbic acid by molecular oxygen. I. Cupric and ferric ion catalyzed oxidation. *J Am Chem Soc* 89:4176–4185. <https://doi.org/10.1021/ja00992a036>
- Uchida K (2003) Histidine and lysine as targets of oxidative modification. *Amino Acids* 25:249–257. <https://doi.org/10.1007/s00726-003-0015-y>
- Wang T, Markham A, Thomas SJ, Wang N, Huang L, Clemens M, Rajagopalan N (2019) Solution stability of poloxamer 188 under stress conditions. *J Pharm Sci* 108:1264–1271. <https://doi.org/10.1016/j.xphs.2018.10.057>
- Winterbourn CC (1995) Toxicity of iron and hydrogen peroxide: The fenton reaction. *Toxicol Lett* 82:969–974. [https://doi.org/10.1016/0378-4274\(95\)03532-x](https://doi.org/10.1016/0378-4274(95)03532-x)
- Yao J, Dokuru DK, Noestheden M, Park SS, Kerwin BA, Jona J, Ostovic D, Reid DL (2009) A quantitative kinetic study of polysorbate autoxidation: the role of unsaturated fatty acid ester substituents. *Pharm Res* 26:2303–2313. <https://doi.org/10.1007/s11095-009-9946-7>
- Zepp RG, Faust BC, Holgné J (1992) Hydroxyl radical formation in aqueous reaction (pH 3–8) of iron (II) with hydrogen peroxide: the photo-fenton reaction. *Environ Sci Technol* 26:313–319. <https://doi.org/10.1021/es00026a011>
- Zhang L, Yadav S, Wang YJ, Mozziconacci O, Schöneich C (2018) Dual effect of histidine on polysorbate 20 stability: mechanistic studies. *Pharm Res* 35:33. <https://doi.org/10.1007/s11095-017-2321-1>

## Publisher's Note

Springer Nature remains neutral with regard to jurisdictional claims in published maps and institutional affiliations.